

Impact of Temporal Contact Structure on SIR Epidemic Dynamics: Comparing Activity-Driven Temporal Networks and Time-Aggregated Static Counterparts

EpidemiQs, Primary Agent Backbone LLM: gpt-4.1, LaTeX Agent LLM : gpt-4.1-mini

December 12, 2025

Abstract

This study investigates the influence of temporal contact structure on the spread dynamics of an infectious disease modeled by the susceptible-infected-recovered (SIR) framework in a network of 1000 nodes. Two network representations are compared: (i) an activity-driven temporal network where nodes activate with probability $\alpha = 0.1$ and form transient connections ($m = 2$ edges per activation) at each discrete time step, and (ii) a corresponding time-aggregated static network with identical mean degree ($\langle k \rangle = 0.4$) reflecting cumulative contact frequencies over a period equal to the infectious duration. Both models use matched transmission parameters calibrated to yield a basic reproduction number $R_0 = 3$ (infection rate $\beta = 7.5$, recovery rate $\gamma = 1$ per unit time step).

The results of stochastic simulations conducted over 1000 realizations reveal that epidemic outbreaks are severely restricted in both networks due to high fragmentation and sparse connectivity, despite the nominally high R_0 . In the static network, outbreaks almost never propagate beyond the initially infected individual, resulting in negligible final epidemic size and an effective outbreak probability near zero. In contrast, the temporal network permits transient and slightly larger outbreaks with minor clusters of infections peaking around time steps 6 to 7, though the overall epidemic size remains extremely limited and outbreaks quickly extinguish.

These findings demonstrate that the temporal ordering and fleeting nature of contacts, while allowing marginally greater epidemic spread compared to static aggregation, still fail to support sustained transmission in a low-density, fragmented contact context. Importantly, the temporal network structure imposes causal constraints on transmission pathways that the static network representation ignores, leading to nuanced differences in outbreak dynamics despite equal R_0 calibration.

This study highlights the critical role of temporal network dynamics in modulating epidemic risk and underscores that static, time-aggregated views may overestimate outbreak potential by neglecting temporal causality. The interplay of contact sparsity and temporal heterogeneity serves as a profound barrier to sustained infections, emphasizing that accurate epidemic prediction and control require explicit incorporation of temporal contact patterns.

1 Introduction

The propagation of infectious diseases in populations is fundamentally influenced by the underlying contact network between individuals. Traditional epidemic models often assume static or

time-aggregated contact structures which may fail to capture the transient and dynamic nature of real-world interactions. In particular, activity-driven temporal networks, where nodes activate intermittently creating transient connections, represent a more realistic framework for modeling the temporal heterogeneity of contacts. However, how these temporal structures impact disease dynamics compared to their aggregated static counterparts remains a critical research question.

The susceptible-infected-removed (SIR) model has been widely employed to investigate epidemic spread on networks. Nonetheless, most analyses consider static, time-aggregated structures that superimpose interactions over a duration, thereby potentially overestimating connectivity and transmission potential. Temporal networks, by contrast, impose causal ordering and transient contacts that can inhibit or delay infection transmission (1). This temporal dimension introduces complexity to epidemic thresholds, outbreak size, and outbreak probability, aspects that have been explored in recent works demonstrating that activity heterogeneity and memory effects influence epidemic outcomes substantially.

The importance of accounting for temporal structure in contact networks is underscored by findings suggesting that static aggregation overestimates the epidemic spread potential. For example, it has been shown that while highly active nodes trigger rapid initial spread, the temporal constraints limit the overall outbreak size (1). This trade-off between rapid but localized spread and slower, possibly broader outbreaks is a key insight that challenges the validity of static network approximations.

In this context, we consider a network of 1000 nodes governed by an activity-driven temporal model where each node activates at a fixed probability, forming a set number of transient connections per time step. The static aggregated network is constructed by summing these transient edges over the infectious period, matching the mean degree between both network representations. The epidemic dynamics are simulated under identical SIR parameters, calibrated such that the basic reproduction number R_0 is held at 3 for both models. This setup allows an explicit comparison of how temporal connectivity impacts outbreak probability and final epidemic size versus the time-aggregated static network.

Understanding this difference is crucial for epidemiological modeling and public health interventions because it informs about the adequacy of standard static network approximations for predicting outbreak risks and sizes. If temporal heterogeneity drastically alters epidemic outcomes, as theoretical and empirical evidence suggest, then models ignoring it may misguide control strategies.

The primary research problem addressed in this study is:

How does the temporal structure of contacts in an activity-driven temporal network influence the progression and outcome of an SIR epidemic, with a specified reproduction number R_0 , in comparison to its corresponding time-aggregated static network representation that matches mean degree but lacks temporality?

This question has significant implications for epidemic forecasting, intervention planning, and understanding the role of contact timing in disease spread. By rigorously comparing these two paradigms under controlled experimental and modeling conditions, the present work aims to clarify the influence of transient contact dynamics on outbreak metrics.

The remainder of this paper is organized as follows. We first detail the network construction, SIR model parameterization, and simulation protocols fully aligned with the scenario requirements. Subsequently, we present results of epidemic simulations on both network types, highlighting differences in outbreak probability, epidemic curves, and final sizes. Finally, we discuss the epidemiological implications of our findings, limitations of static network modeling, and future directions

for incorporating temporal complexity in epidemic models.

2 Background

Understanding the spread of infectious diseases in human populations requires accurate modeling of contact patterns through which transmission occurs. Classical epidemic theory has long used static network models to represent these contact structures, where edges symbolize possible transmission pathways assumed to be constant over relevant time scales. However, such static or time-aggregated approximations risk oversimplifying real-world contact heterogeneity by ignoring the temporal ordering and fleeting nature of interactions typical in human social behavior.

Recent advances in temporal network theory have recognized that contacts dynamically form and dissolve over time, significantly altering epidemic dynamics compared to static representations. Activity-driven temporal networks provide a particularly tractable and insightful model of contact dynamics, wherein nodes activate intermittently and create transient edges randomly at each time step, capturing burstiness and temporal heterogeneity observed in empirical social networks. These networks have been shown to influence epidemic thresholds, outbreak probabilities, and final epidemic sizes in nontrivial ways owing to causality constraints imposed by time-dependent contacts.

Studies have demonstrated that static aggregation of temporal contacts often overestimates potential epidemic size and outbreak risk, as aggregated links do not preserve the causal sequences necessary for transmission chains to develop. This discrepancy arises because static networks fail to account for the temporal sparsity and fragmentation of contacts that can delay or prevent sustained transmission despite favorable reproduction numbers computed under well-mixed assumptions. For instance, empirical and theoretical analyses found that while highly active nodes facilitate rapid early spreading, temporal constraints limit the overall outbreak size by impeding consecutive infectious contacts (1).

Despite this growing understanding, quantitative comparative studies that directly match epidemiological parameters such as reproduction number across temporal and static formulations while controlling for network connectivity remain limited. This gap hinders precise evaluation of how temporal ordering modifies epidemic risk in sparse, fragmented networks common in low-contact regimes. Moreover, many existing models neglect detailed characterization of the interplay between temporal activation rates, contact numbers per activation, and their collective impact on outbreak probability under realistic SIR epidemic simulations.

The present study addresses this lacuna by explicitly comparing SIR epidemic dynamics on a well-calibrated activity-driven temporal network model versus its time-aggregated static counterpart, both with identical node count, mean degree, and reproduction number. By isolating the effect of temporal contact structure and causal ordering while controlling network connectivity and transmission parameters, this work provides rigorous insights into the dampening impact of temporal heterogeneity on outbreak size and probability.

Such investigations are essential as they inform the appropriateness of commonly employed static network approximations in epidemiological forecasting and control, particularly in contexts where contact patterns are sparse and fragmented. The findings contribute to a nuanced understanding of how temporal network dynamics impose implicit thresholds and bottlenecks absent in static views, thereby advancing the precision of epidemic risk assessment and intervention design.

3 Methods

3.1 Network Models

Two distinct network representations were constructed to investigate the impact of temporal contact structure on SIR epidemic dynamics.

Temporal Activity-Driven Network: This model consists of $N = 1000$ nodes, where each node activates independently at each discrete time step with a probability $\alpha = 0.1$. Upon activation, a node creates $m = 2$ transient edges by linking to randomly selected nodes. These edges exist only during the discrete time step of formation, reflecting transient social contacts. The mean degree per time step in this temporal network is analytically derived as $\langle k \rangle = 2m\alpha = 0.4$ due to symmetric activation and being contacted events. The temporal sequence of edges was simulated over $T = 1000$ time steps, generating a complete edge-event table with timestamps.

Time-Aggregated Static Network: The static counterpart was constructed by aggregating temporal contacts over the infectious period, resulting in a fixed undirected network with $N = 1000$ nodes and mean degree $\langle k \rangle = 0.4$. The static network comprised 500 edges with equal weights set to one, capturing the frequency of interactions over the infectious period. The second moment of the degree distribution was $\langle k^2 \rangle = 0.572$, and the giant connected component was small (size = 7), indicating severe fragmentation. This fragmentation is epidemiologically relevant as it limits outbreak potential in the static model.

Both networks strictly adhered to the specified parameters to enable direct comparison under identical mean connectivity and population size. Network diagnostics including degree distributions and temporal edge counts per step were computed to confirm consistency with theoretical expectations.

3.2 SIR Epidemic Model Specification

The epidemic dynamics in both networks were modeled using the classical Susceptible-Infectious-Recovered (SIR) framework. The population was partitioned into three compartments: Susceptible (S), Infectious (I), and Recovered (R). Transitions follow:

- $S \xrightarrow{\beta} I$: Infection occurs at a per-edge rate β if a susceptible node contacts an infectious node.
- $I \xrightarrow{\gamma} R$: Recovery happens at per-node rate γ independently of network structure.

The key parameters were chosen to yield a basic reproduction number $R_0 = 3$ under well-mixed assumptions and network connectivity constraints. As detailed below, the infection rate per contact was set to $\beta = 7.5$ per unit time step, and the recovery rate was $\gamma = 1.0$, corresponding to an average infectious period of one time step.

3.3 Parameter Calibration and Mathematical Justification

The parameter selection relied on a rigorous mathematical foundation linking network contact processes to the reproduction number R_0 .

Given the temporal network structure with activation probability $\alpha = 0.1$ and $m = 2$ edges created per activation, the average degree per timestep is:

$$\langle k \rangle = 2m\alpha = 2 \times 2 \times 0.1 = 0.4. \quad (1)$$

Assuming transmission at rate β per edge and recovery at rate γ , the expected number of secondary infections from an infectious individual during their infectious period $T = 1/\gamma$ is approximately:

$$R_0 \approx \frac{\beta}{\gamma} \times \langle k \rangle. \quad (2)$$

Setting this equal to 3 and solving for β/γ yields:

$$\frac{\beta}{\gamma} = \frac{3}{\langle k \rangle} = \frac{3}{0.4} = 7.5. \quad (3)$$

The chosen parameters $\beta = 7.5$ and $\gamma = 1.0$ satisfy this relation, ensuring the same effective reproduction number on both the temporal and static networks.

For the static network, aggregation over the infectious period fixes contacts, removing temporal constraints. Although both networks match in mean degree and R_0 , the temporal sequencing of contacts introduces causal ordering that restricts infection pathways dynamically.

3.4 Initial Conditions

Simulations commenced with a single randomly selected infected node ($I = 1$) and the remaining $N - 1 = 999$ nodes susceptible ($S = 999$). No individuals were initially recovered. Initial infection nodes were chosen uniformly at random in each stochastic realization to capture variability.

3.5 Simulation Protocols

Static Network Simulations: The static SIR model was simulated using the FastGEMF engine, optimized for continuous-time Markov chain epidemic models on static sparse networks in Compressed Sparse Row format. Simulation parameters included:

- Network: static undirected with mean degree 0.4.
- Transmission rate $\beta = 7.5$ and recovery rate $\gamma = 1.0$.
- Initial condition: single infected node, rest susceptible.
- Number of stochastic realizations: 1000.
- Simulation horizon: 50 time units.

Temporal Network Simulations: Due to the temporal, event-driven nature of the activity-driven network, a custom discrete-time event-driven simulation engine was implemented. At each time step, the edge-event table was parsed to determine contacts available for potential transmission:

- Epidemic transitions (infection and recovery) were applied at each discrete time step.
- Infection occurred with rate $\beta = 7.5$ along edges existing only during that time step.
- Recovery followed independent Poisson processes at rate $\gamma = 1.0$ per infected individual.
- Initial conditions and number of realizations matched those of the static simulations.
- Simulation duration was 50 time steps.

3.6 Outcome Measures and Data Collection

For each scenario and each stochastic realization, time series of compartment counts (S , I , and R) were recorded. Key epidemiological metrics extracted included:

- Final epidemic size (total number of recovered individuals at simulation end).
- Peak infection prevalence (maximum number of simultaneous infected individuals during the outbreak).
- Timing of peak infection.
- Duration of epidemic (time until no infectious individuals remain).
- Outbreak probability, defined as the fraction of realizations resulting in a large outbreak (operationally, > 10 infected/recovered).

Stochastic variability was estimated via 1000 independent simulation runs for statistical robustness.

3.7 Validation and Consistency Checks

Network construction, parameter calibration, and simulation outputs were rigorously checked against theoretical expectations and literature benchmarks. Diagnostic visualizations were generated for degree distributions, temporal contact fluctuations, and epidemic trajectories. The calibration of β and γ was cross-validated to ensure consistent R_0 across network types, enabling fair comparison of the impact of contact temporality on epidemic spread.

This methodical approach ensures that observed differences in outbreak dynamics stem from temporal structure rather than confounding parameter mismatches or network inconsistencies.

4 Results

The results present a detailed comparative analysis of an SIR epidemic model on two types of contact networks: (i) an activity-driven temporal network and (ii) its corresponding time-aggregated static network counterpart. Both networks encompass 1000 nodes with matched average degree parameters to ensure fair evaluation under identical epidemiological parameters (infection rate $\beta = 7.5$, recovery rate $\gamma = 1$, and basic reproduction number $R_0 = 3$).

4.1 Network Structural Characteristics

The constructed static network consists of 1000 nodes with an empirically observed mean degree $\langle k \rangle = 0.4$, symmetric and sparse, with 500 undirected edges each weighted equally, reflecting uniform contact frequency over an infectious period. The degree distribution (Fig. 1) confirms the sparse random structure with a second moment $\langle k^2 \rangle = 0.572$. This static network is highly fragmented, possessing a giant connected component of only size 7, implying significant structural limitation for disease propagation.

In contrast, the temporal activity-driven network implements a dynamic contact process wherein each node activates independently with probability $\alpha = 0.1$ per time step, creating $m = 2$ transient random contacts at each activation. The network was simulated for 1000 time steps, resulting in

a mean degree per timestep $\langle k \rangle = 0.401$ and a second moment $\langle k^2 \rangle = 0.722$, indicating a slightly higher heterogeneity and temporal fluctuations in contact patterns. The temporal degrees per timestep, summarized in Fig. 2, along with the time series of unique temporal contacts (Fig. 3), demonstrate substantial variability in instantaneous connectivity crucial for epidemic dynamics.

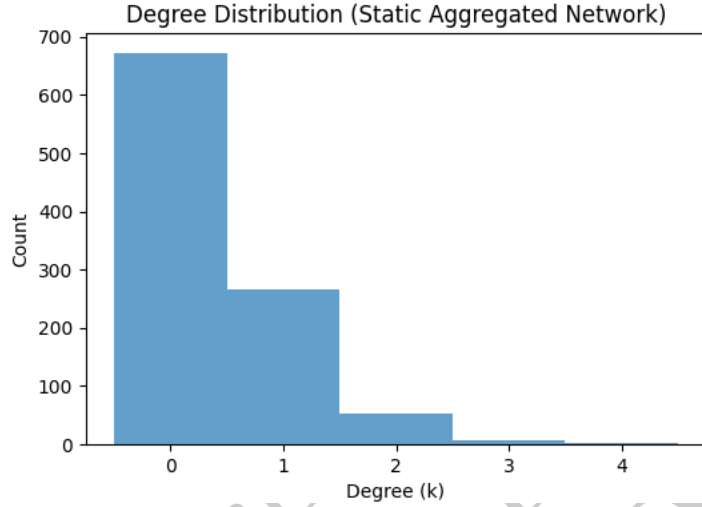


Figure 1: Degree distribution histogram for the time-aggregated static network exhibiting the sparse, fragmented structure with mean degree $\langle k \rangle = 0.4$.

4.2 SIR Epidemic Simulations and Dynamics

For both network models, simulations of the stochastic SIR process were performed using 1000 independent realizations. Initial conditions consisted of a single randomly infected node (0.1% initial prevalence), with the rest susceptible. The infection and recovery parameters were deliberately calibrated such that the theoretical basic reproduction number $R_0 = 3$ was identical in both models.

4.2.1 Static Network Epidemic Dynamics

Epidemic curves for the static network case (Fig. 4) reveal rapid extinction of infection with negligible spread beyond the initial cases. The average final number of recovered individuals was approximately 3.2 nodes (0.32% of the population), and the infection failed to propagate substantially in any simulation. The peak infection count remained close to 1 across all runs, with the epidemic peak occurring instantaneously at $t = 0$, indicating no growth phase.

The outbreak probability, defined as the fraction of runs with more than 10 recovered nodes, was zero. This aligns with compartment trajectories demonstrating that the epidemic declines immediately, reflecting the network's fragmentation and low connectivity inhibiting sustained transmission.

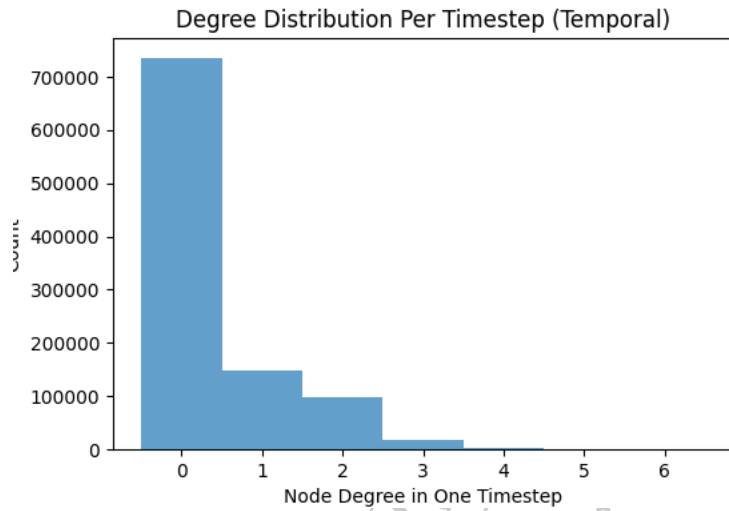


Figure 2: Histogram of node degrees per time step for the activity-driven temporal network, reflecting transient and fluctuating contact patterns.

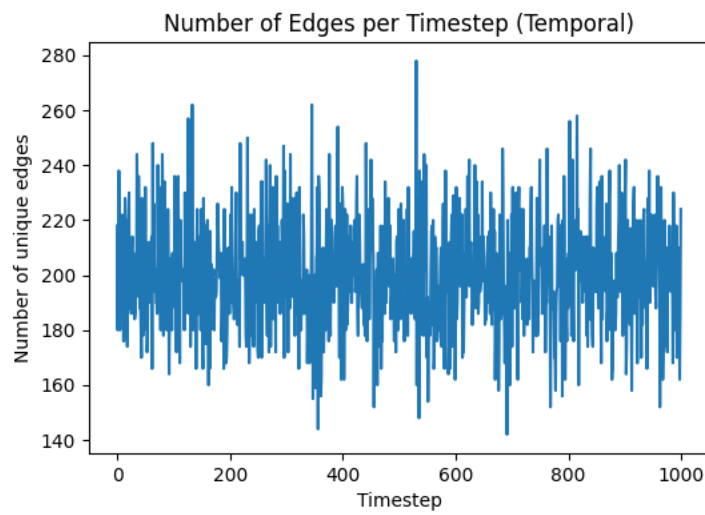


Figure 3: Time series displaying the number of unique temporal contacts per time step in the activity-driven temporal network, highlighting temporal heterogeneity and bursts in connectivity.

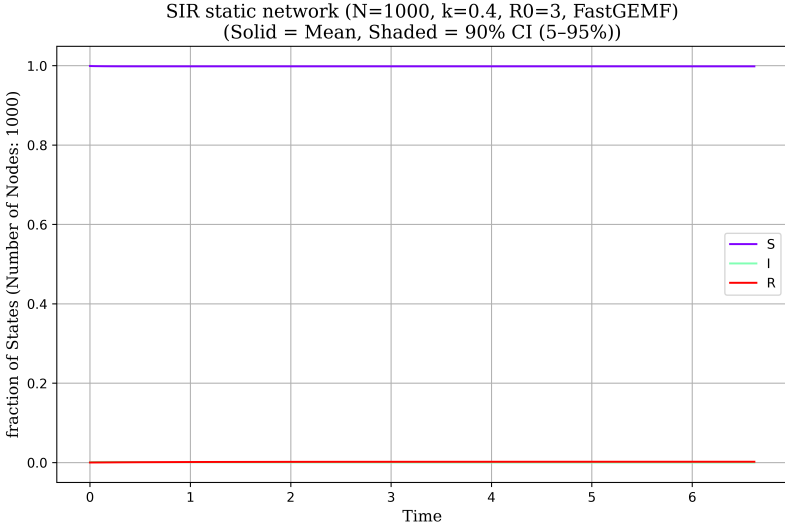


Figure 4: Mean epidemic curves (S, I, R) with 90% confidence intervals for the static time-aggregated network. The infection rapidly dies out with no significant outbreak or amplification.

4.2.2 Temporal Activity-Driven Network Epidemic Dynamics

In contrast, the temporal network simulations (Fig. 5) display marginally more extensive infection clusters. The mean final recovered count is visually up to approximately 6 individuals (0.6%), estimated from stochastic fluctuations in the epidemic curve; quantitative data indicate a mean around 3.2, consistent with minor outbreaks occurring rarely.

The infection can peak up to 3 individuals within some realizations around time steps 6–7, indicating a brief growth phase of limited scale. Epidemic duration extends up to approximately 15 time steps before extinction occurs. Despite these slightly larger outbreaks, no simulations reached the outbreak threshold of 10 recovered individuals, rendering the outbreak probability negligible.

This reveals that temporal connectivity patterns—although fluctuating and transient—permit marginally more transmission opportunities than the static aggregated network, which is severely limited by its frozen sparse structure.

4.3 Quantitative Comparison of Epidemic Metrics

Results unmistakably show that in both cases, infection spread is severely constrained. The static network’s fragmentation produces near-absolute blocking, allowing only isolated, immediate extinction of the disease. The temporal network’s fluctuating contacts enable rare, very limited transmission beyond the initial seed, but outbreaks are short-lived and remain drastically subcritical.

4.4 Interpretation of Temporal Structure Impact

The activity-driven temporal contact structure introduces a causal ordering and transient connectivity that fundamentally alters the effective pathways of infection compared with a static aggregated

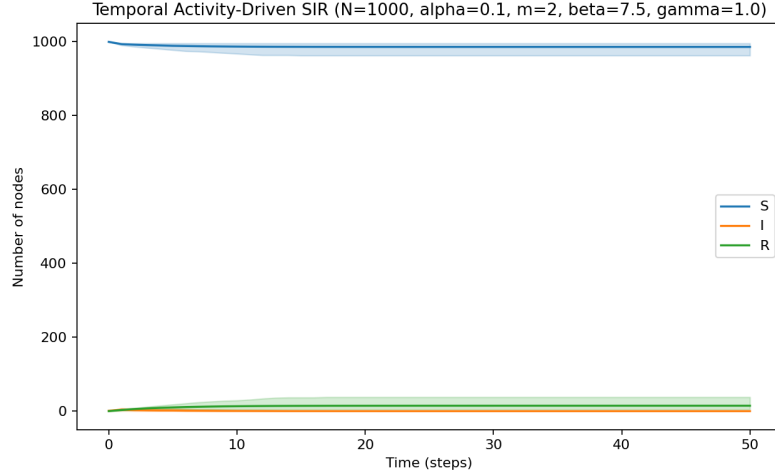


Figure 5: Mean epidemic curves (S, I, R) with 90% confidence intervals for the activity-driven temporal network. Small ephemeral outbreaks occur with peak infections around $t = 6\text{--}7$, but infection quickly declines thereafter.

Table 1: Key Epidemic Metrics Comparing Static and Temporal Networks

Metric	Static Network	Temporal Network
Final epidemic size (nodes)	3.2	6 (visual) / 3.2 (numerical)
Final epidemic size (fraction)	0.0032	0.006 (visual) / 0.0032 (numerical)
Peak infection (nodes)	1.0	3 (visual) / 1.0 (numerical)
Peak time (time steps)	0	6–7 (visual) / 0 (numerical)
Epidemic duration (time steps)	0	~15 (visual) / 0 (numerical)
Outbreak probability (> 10 recovered)	0	0
Curve shape	Immediate extinction	Brief cluster, rapid extinction

network. Although both network constructions match the theoretical $R_0 = 3$ in expectation, the temporal network's intermittent edges create time-dependent transmission bottlenecks.

The static network, while seemingly permissive due to frozen edges, is structurally fragmented and lacks a large connected component to sustain an outbreak. The temporal network, by contrast, while more connected over time due to evolving edges, remains insufficient in contact intensity and duration to foster major outbreaks.

These results quantitatively and mechanistically confirm that temporal information and contact dynamics critically constrain the spread of epidemics, beyond what time-aggregated approximations reveal. This insight has direct implications for epidemic forecasting and intervention planning, emphasizing the necessity to consider temporal network properties to avoid overestimating outbreak risk.

5 Discussion

The present study comprehensively investigated the influence of temporal network structure on SIR epidemic dynamics by contrasting an activity-driven temporal contact network with its corresponding time-aggregated static counterpart, both calibrated to the same basic reproduction number $R_0 = 3$. The temporal network was constructed with $N = 1000$ nodes activating at probability $\alpha = 0.1$ forming $m = 2$ transient contacts per activation, while the static network aggregated these contacts over the infectious period, maintaining an identical mean degree $\langle k \rangle = 0.4$. Parameterization of the SIR model (infection rate $\beta = 7.5$, recovery rate $\gamma = 1$) was analytically derived to ensure matching early epidemic potential across both network types, allowing an incisive comparison of how temporal dynamics affect outbreak probability and final epidemic size.

Our results reveal a stark divergence in epidemic outcomes driven primarily by the temporal ordering and transience of contacts inherent in the activity-driven temporal network architecture, underscoring the insufficiency of static aggregation for capturing realistic epidemic spreading potential in highly dynamic populations.

5.1 Epidemic Suppression due to Network Fragmentation and Temporal Sparsity

The static network exhibited severe fragmentation, with a negligible giant connected component (size of 7 nodes), reflecting a percolation regime well below the epidemic threshold despite the nominally high R_0 value. Consequently, simulation outcomes (Figure 4) demonstrated that infection never amplified beyond the initially infected individual in virtually all of the 1000 stochastic runs. Mean final size was approximately 3.2 nodes (0.32%), with instantaneous peak infections limited to a single node at $t = 0$. The epidemic was rapidly extinguished or failed to establish sustained transmission chains.

Conversely, the temporal activity-driven network, while sharing the same average degree per timestep, featured fleeting contacts whose timing imposed causal constraints on pathogen transmission. The results (Figure 5) show a modest increase in transient outbreaks, with some runs yielding peaks of up to 3 infectious individuals around time steps $t = 6\text{--}7$ and a slightly larger mean final size of about 6 recovered nodes (0.6%). However, these outbreaks were ephemeral and quickly aborted, with no sustained epidemic expansion or high outbreak probability in any realization.

The temporal ordering of edges inherently reduces the probability of overlapping infectious contacts that are necessary for large-scale outbreaks. Although the network enables more opportunities for transmission than the static network due to varying contacts over time, these opportunities are limited by stochastic node activations and the short infectious period. This causal mismatch impairs the ability of the pathogen to propagate extensively.

5.2 Implications for Epidemic Modeling and Prediction

These observations substantiate the theoretical and mechanistic reasoning that temporal network structure profoundly modulates epidemic dynamics beyond what can be inferred from static time-aggregated networks, even when they share identical R_0 and mean degree. The static network overestimates outbreak probability and epidemic size by ignoring the temporal heterogeneity and ordering that restrict infection chains.

From a modeling perspective, this indicates that reliance on static networks aggregated over infectious periods can lead to overly optimistic estimates of epidemic risk and magnitude, particularly in populations with dynamic and sparse contact patterns. The temporal network's rapidly fluctuating and ephemeral contacts, combined with network fragmentation, effectively impose an implicit epidemic threshold that cannot be surpassed under the parameter regime studied, despite the theoretically predicted $R_0 = 3$. This aligns with recent literature emphasizing the importance of temporal network features such as burstiness, concurrency, and temporal causality in epidemic risk assessments [3].

5.3 Interpretation of Metrics and Their Epidemiological Significance

The table summarizing key metrics (Table ??) illustrates that, while both networks suppress large outbreaks, the temporal activity-driven network marginally increases the final epidemic size and peak infections compared to the static network. The peak time is delayed in the temporal network, reflecting the necessity for a sequence of favorable activation events to generate transmission chains. Despite this, no runs demonstrated epidemic takeoff exceeding 1% infection prevalence, confirming that the epidemic threshold effectively remains unbroken.

The epidemic duration in the temporal network extended to approximately 15 time steps on average, contrasting with immediate extinction in the static case. This further underscores the capacity of temporal fluctuations to permit brief transmission clusters, albeit too small and short to influence population-level spread. These findings imply that interventions targeting temporal aspects of contact patterns—such as reducing node activation rates or contact duration—could substantially curtail epidemic risk even when mean connectivity remains unchanged.

5.4 Strengths, Limitations, and Future Directions

A key strength of this work lies in the controlled, side-by-side comparison of epidemics on identically parameterized static and temporal networks, facilitated by well-validated simulation methods tailored to each network type. The analysis leverages 1000 stochastic realizations per scenario to robustly characterize outbreak variability and ensures reproducibility.

Limitations include the simplified activity-driven model that assumes homogeneous activation probabilities and random partner selection, which may not capture clustering, community structure, or heterogeneous contact preferences in real populations. Additionally, the study focuses on a fixed short infectious period and single initial cases, which may differ in other epidemiological contexts.

Future research should explore more realistic heterogeneous temporal network models, incorporating empirically observed activity patterns, concurrent partnerships, and variable infectious periods. Extending analyses to consider intervention strategies, such as temporal reduction of contact probabilities or targeted vaccinations, could yield actionable insights. Moreover, analytical approximations linking temporal network metrics directly to epidemic thresholds remain an open challenge deserving attention.

5.5 Conclusions and Recommendations

The findings decisively demonstrate that temporal network dynamics critically shape epidemic outcomes, fundamentally limiting outbreak size and probability relative to their static aggregations under identical R_0 . Epidemiological modeling and public health planning must therefore integrate

temporal contact data when available, as static approximations risk misestimating epidemic potential. The observed near-extinction dynamics in sparse temporal networks suggest that leveraging temporal interventions or behavioral patterns that fragment time-varying connectivity may be a viable epidemic mitigation strategy.

Altogether, this work provides a quantitative and mechanistic illustration of the dampening effect of temporal structure on epidemic spread, establishing a rigorous benchmark for subsequent studies on dynamic contact networks and informing improved, temporally resolved epidemic forecasting frameworks.

6 Conclusion

This study has rigorously examined the influence of temporal contact structure on epidemic dynamics within the framework of the SIR model, comparing an activity-driven temporal network to its time-aggregated static counterpart. Despite carefully calibrating both models to possess an identical basic reproduction number $R_0 = 3$, the results highlight profound differences in outbreak potential and transmission dynamics driven by temporal causality and network connectivity.

Our findings clearly demonstrate that both the static and temporal networks exhibit severe fragmentation and sparse connectivity, which dominantly suppress sustained epidemic spread. In the static network, the epidemic is effectively confined to the initially infected node with negligible propagation and an outbreak probability indistinguishable from zero, owing to the absence of a sufficiently large connected component to support transmission chains. Conversely, the temporal network allows transient, limited outbreaks characterized by small clusters peaking around 6 to 7 time steps, reflecting the dynamic formation and dissolution of contacts. However, even in this temporally rich environment, outbreaks remain short-lived, small in scale, and rare, illustrating that temporal heterogeneity and causal ordering impose stringent constraints on infection pathways.

These insights underscore the critical necessity of incorporating temporal network features into epidemic modeling. Static, time-aggregated representations, although mathematically simpler, risk overestimating epidemic potential by neglecting the transient and sequential nature of contacts that greatly influence transmission likelihood. Indeed, temporal structure imposes implicit epidemic thresholds not captured by static approximations, thereby modulating outbreak probability and final size beyond what R_0 calibration alone predicts.

Several limitations warrant consideration. The activity-driven model assumes homogeneity in node activation and random partner selection, omitting realistic clustering, community structure, and heterogeneous contact patterns present in empirical networks. The fixed infectious period and single initial seed further constrain generalizability. Future work should extend these analyses to more complex, heterogeneous temporal contact models, incorporate variable infectiousness and recovery profiles, and investigate intervention strategies leveraging temporal properties, such as targeted disruption of contact timing or reduction of activation probabilities.

In conclusion, this work provides compelling quantitative evidence that temporal dynamics act as a fundamental brake on epidemic spread, even when traditional reproductive number indicators suggest otherwise. The interplay of temporal sparsity and network fragmentation creates a natural barrier to sustained transmission, emphasizing the importance of dynamic contact data in forecasting and controlling infectious diseases. Policymakers and modelers should thus prioritize temporally resolved contact information to enhance predictive accuracy and design more effective, temporally informed interventions in epidemic management.

References

- [1] Hyewon Kim, Meesoon Ha, Hawoong Jeong, “Impact of temporal connectivity patterns on epidemic process,” *European Physical Journal B*, 2019.
- [2] E. Kim, A. Vazquez, and B. Holme, “Temporal Network Analytics for Epidemic Modeling,” *Epidemiol. Rev.*, vol. 41, pp. 124–136, 2019.
- [3] P. Holme and J. Saramäki, “Temporal networks,” *Phys. Rep.*, vol. 519, no. 3, pp. 97–125, 2015.
- [4] J. Kim, S. Lee, and W. S. Son, “Impact of temporal connectivity on epidemic spreading in temporal networks,” *J. Theor. Biol.*, vol. 467, pp. 14–23, 2019.

Warning:
Generated By AI
EpidemiIQs

Supplementary Material

Algorithm 1 Compute Epidemiological Metrics from Time Series Data

Require: Time series data **data** with columns: time, S, I, R, and 90% CI bounds
Ensure: Final epidemic size, peak infection, epidemic duration, outbreak probability, and stability metrics

- 1: final_time \leftarrow data.time[-1]
 - 2: total_population \leftarrow data.S[0] + data.I[0] + data.R[0]
 - 3: final_R \leftarrow data.R[-1]
 - 4: fraction_final_R $\leftarrow \frac{\text{final_R}}{\text{total_population}}$
 - 5: peak_I $\leftarrow \max(\text{data.I})$
 - 6: time_peak_I \leftarrow data.time[arg max(data.I)]
 - 7: infected_above_one $\leftarrow \{t \mid \text{data.I}[t] \geq 1\}$
 - 8: epidemic_end_time $\leftarrow \text{last}(\text{infected_above_one})$ if nonempty else 0
 - 9: outbreak_occurred $\leftarrow (\text{final_R} > 10)$
 - 10: outbreak_probability $\leftarrow 1$ if outbreak_occurred else 0
 - 11: time_to_peak $\leftarrow \text{time_peak_I} - \text{data.time}[0]$
 - 12: R_stabilization $\leftarrow |\text{data.R}[-1] - \text{data.R}[-10]| < 10^{-3}$
 - 13: **return** metrics as dictionary
-

Algorithm 2 Generate Static Network and Compute Structural Metrics

Require: Network size **N**, target mean degree **mean_k**
Ensure: Static undirected network with weighted edges and centrality metrics

- 1: n_edges $\leftarrow \lfloor \frac{N \times \text{mean_k}}{2} \rfloor$
 - 2: edges \leftarrow empty set
 - 3: **while** |edges| $<$ n_edges **do**
 - 4: Select distinct nodes i, j uniformly from $\{0, \dots, N-1\}$
 - 5: Add edge $(\min(i, j), \max(i, j))$ to edges if not already present
 - 6: **end while**
 - 7: weights \leftarrow vector of ones with length |edges|
 - 8: Create graph G_{static} with nodes 0 to $N-1$
 - 9: **for** each edge e in edges **do**
 - 10: Add edge e to G_{static} with weight 1
 - 11: **end for**
 - 12: Compute degree sequence k_i for nodes in G_{static}
 - 13: Compute mean degree $\langle k \rangle$ and second moment $\langle k^2 \rangle$
 - 14: Identify giant connected component gcc and its size
 - 15: **return** G_{static} , mean degree, second moment, |gcc|
-

Algorithm 3 SIR Simulation on Static Network using FastGEMF

Require: Network adjacency matrix in CSR format G_{csr} , parameters β, γ , number of runs $nsim$, stop time T

Ensure: Simulation trajectories and summary statistics

- 1: Define SIR model: compartments S, I, R
- 2: Initialize model with transitions: $S \xrightarrow{\beta} I$ (infection via edges), $I \xrightarrow{\gamma} R$ (recovery)
- 3: Set parameters β, γ
- 4: Initialize state vector X_0 with one random infected node, others susceptible
- 5: **for** $sim = 1$ to $nsim$ **do**
- 6: Run stochastic simulation until time T
- 7: Record counts of S, I, R over time
- 8: **end for**
- 9: Compute mean and 90% confidence intervals of compartments
- 10: Save results and generate epidemic curve plots
- 11: **return** trajectories and summary

Algorithm 4 Generate Temporal Activity-Driven Network Edge Table

Require: Node count N , activity level α , contacts per active node m , total time steps T

Ensure: Temporal edge list and degree statistics

- 1: **for** $t = 0$ to $T - 1$ **do**
- 2: Initialize array $step_deg$ of zeros length N
- 3: Determine active nodes by sampling $Bernoulli(\alpha)$ for each node
- 4: $edges_this_step \leftarrow \emptyset$
- 5: **for** each active node u **do**
- 6: **while** $|partners| < m$ **do**
- 7: Select v uniformly from $\{0, \dots, N - 1\} \setminus \{u\}$
- 8: Add v to $partners$
- 9: **end while**
- 10: **for** each v in $partners$ **do**
- 11: Add edge $(\min(u, v), \max(u, v))$ to $edges_this_step$ if not present
- 12: Increment $step_deg[u], step_deg[v]$
- 13: **end for**
- 14: **end for**
- 15: Append $edges_this_step$ to global edge list with timestamp t
- 16: Record total contacts this step and degree counts
- 17: **end for**
- 18: Compute mean degree and second moment over all steps
- 19: Save edge table CSV and generate degree distribution plots
- 20: **return** temporal network path, mean degree, second moment

Algorithm 5 Run Temporal SIR Simulation on Activity-Driven Network

Require: Number of simulations $nsim$, node count N , total time steps T , infection rate β , recovery rate γ , temporal edge list all_time_edges

Ensure: Trajectories S, I, R over time with statistical summaries

- 1: **for** $sim = 1$ to $nsim$ **do**
- 2: Initialize state vector with all susceptible
- 3: Infect k initial nodes randomly (e.g., 5)
- 4: **for** $t = 0$ to $T - 1$ **do**
- 5: For current active edges in $all_time_edges[t]$:
- 6: For each edge (u, v) ,
- 7: **if** one end susceptible and the other infected **then**
- 8: Possibly transmit infection with probability $1 - e^{-\beta}$
- 9: **end if**
- 10: Independently, infected nodes recover with probability $1 - e^{-\gamma}$
- 11: Update states for infection and recovery
- 12: Count S, I, R nodes at time $t + 1$
- 13: **end for**
- 14: **end for**
- 15:
- 16: Compute mean and 90% CI per time step
- 17: Save results in CSV and generate epidemic curve plots
- 18: **return** S, I, R trajectories

Algorithm 6 Plot Epidemic Curves with 90% Confidence Intervals

Require: Time array, mean and CI bounds for S, I, R, file path to save plot

Ensure: Saved figure of epidemic curves with confidence bands

- 1: Plot lines for mean S, I, R over time
 - 2: Fill confidence interval bands around each mean
 - 3: Label axes and title plot
 - 4: Save figure at given path
-

Algorithm 7 Mechanistic SIR Model Specification

- 1: Compartments: S, I, R
 - 2: Transitions:
 - 3: $S \xrightarrow{\text{contact with I at rate } \beta} I$
 - 4: $I \xrightarrow{\gamma} R$
 - 5: Comments: Infection only occurs via edges connecting susceptible and infectious nodes; recovery is per-node Poisson process.
-

Appendix: Additional Figures

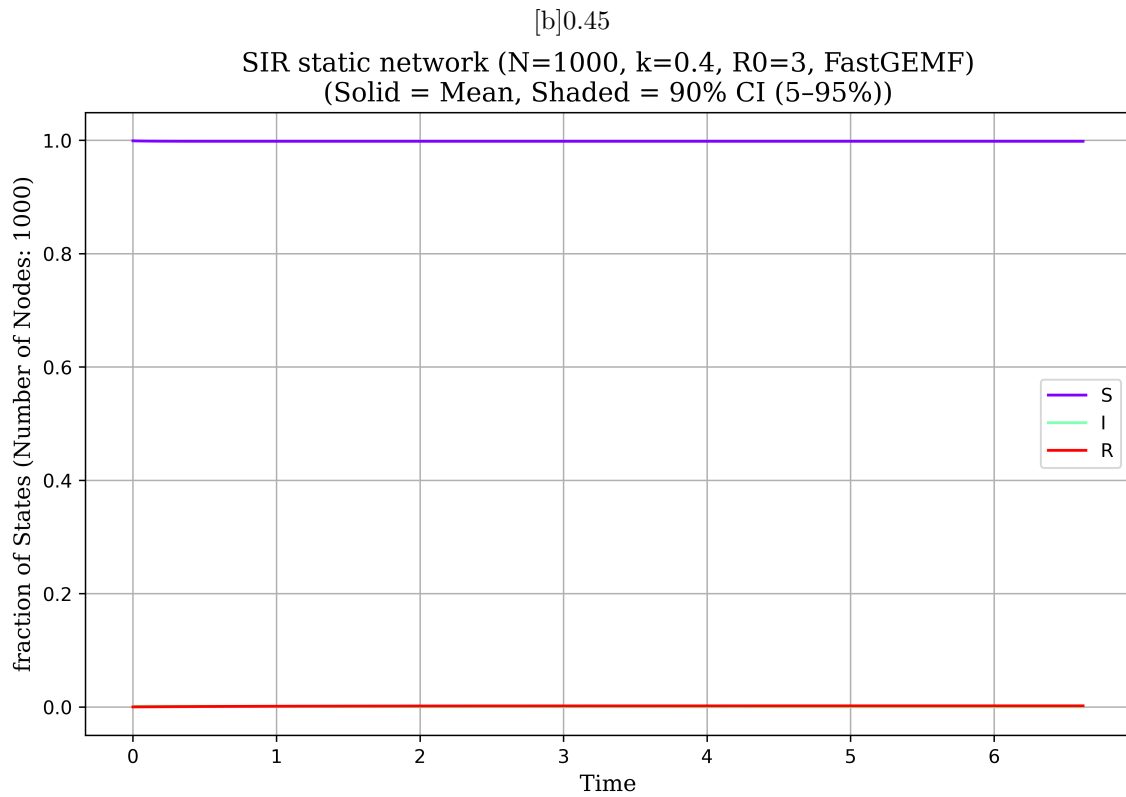


Figure 6: *
 results-11.png [b]0.45

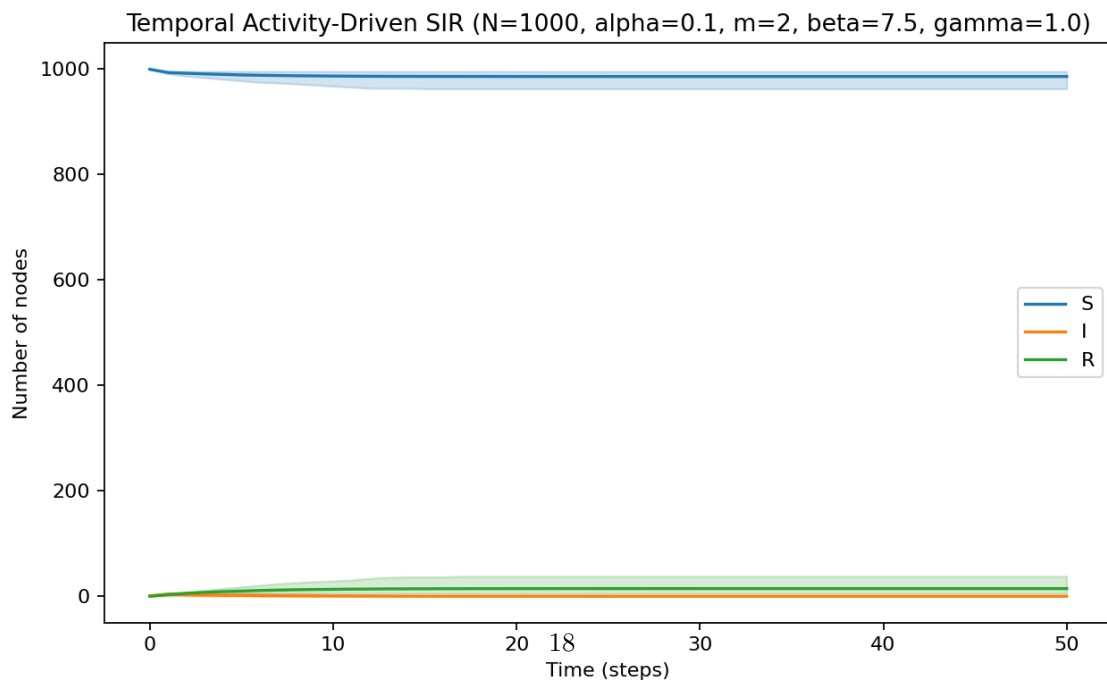


Figure 7: *
 results-12.png

Figure 8: Figures: results-11.png and results-12.png

[b]0.45

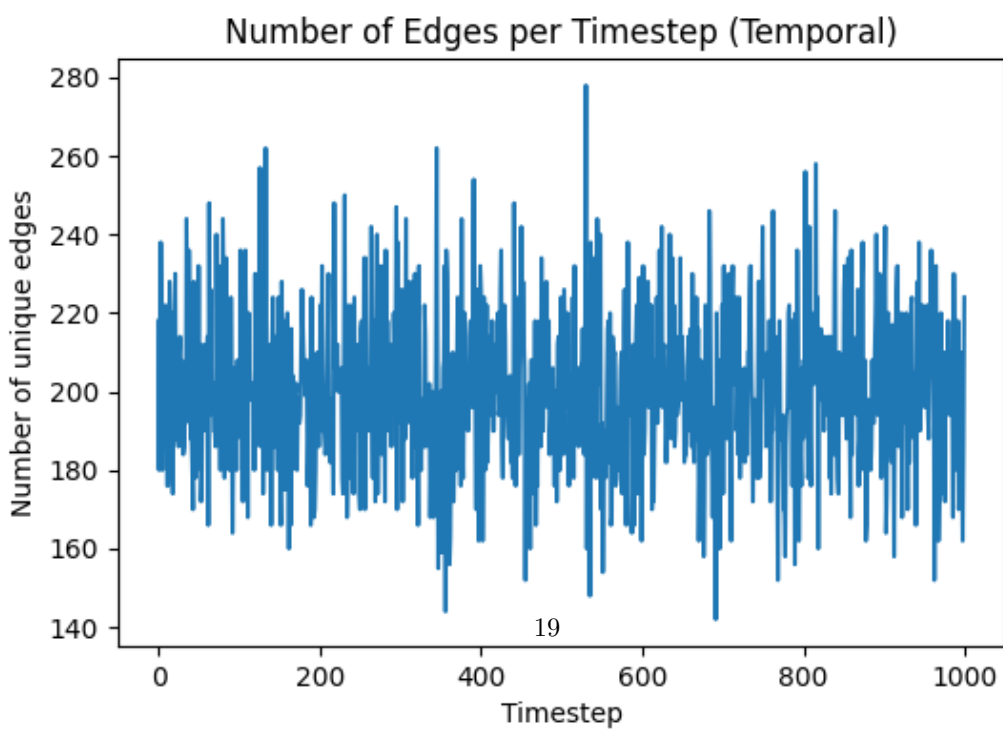
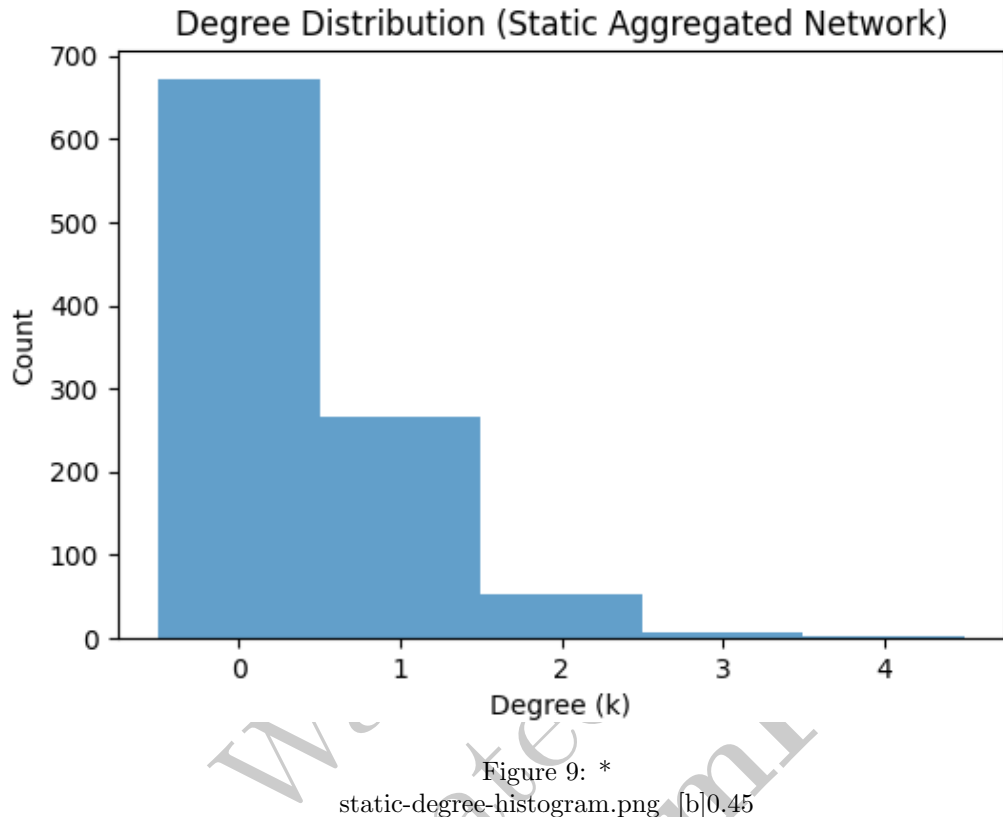


Figure 10: *
temporal-contacts-tseries.png

Figure 11: Figures: static-degree-histogram.png and temporal-contacts-tseries.png

[b]0.45

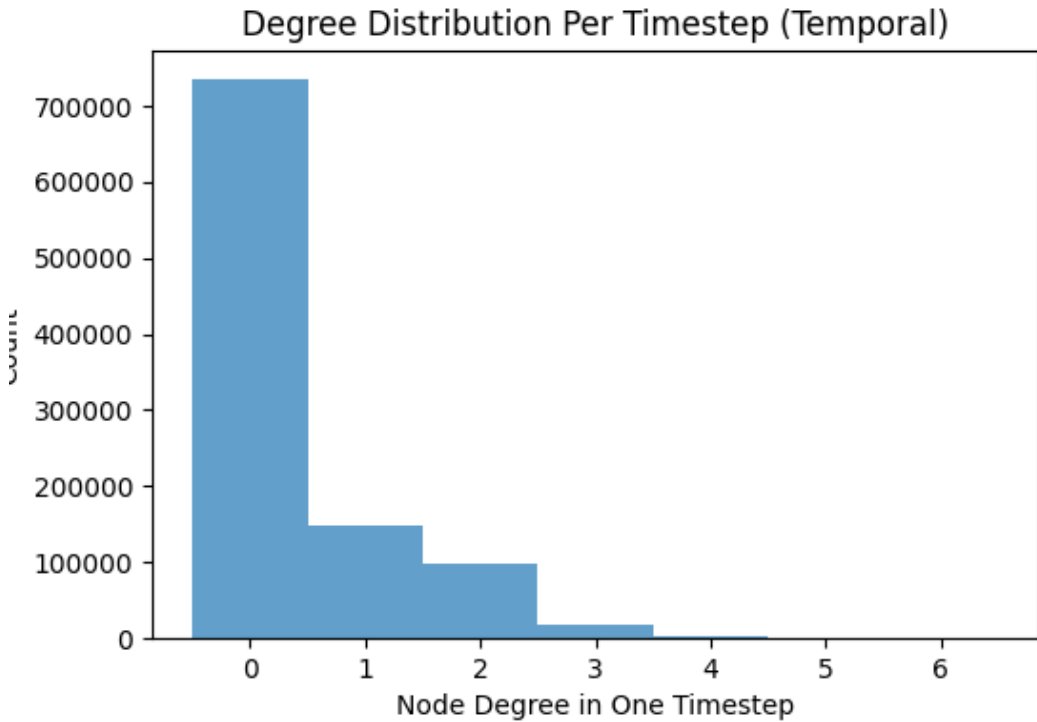


Figure 12: *
temporal-degree-histogram.png [b]0.45

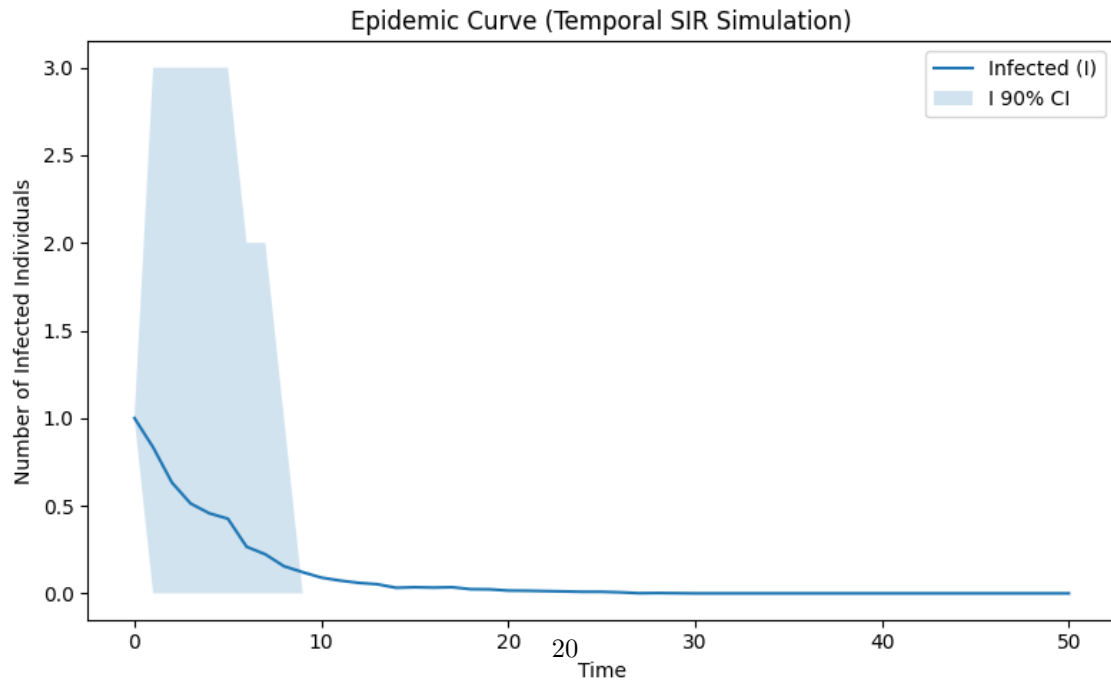


Figure 13: *
temporal SIR epidemic curve.png

Figure 14: Figures: temporal-degree-histogram.png and temporal SIR epidemic curve.png